



**HAL**  
open science

# SPRAY-DRIED CHITOSAN-METAL MICROPARTICLES FOR CIPROFLOXACIN ADSORPTION: KINETIC AND EQUILIBRIUM STUDIES

Franceline Reynaud, Nicolas Tsapis, Michel Deyme, Tibiriça Vasconcelos,  
Claire Gueutin, Sílvia Guterres, Adriana Pohlmann, Elias Fattal

► **To cite this version:**

Franceline Reynaud, Nicolas Tsapis, Michel Deyme, Tibiriça Vasconcelos, Claire Gueutin, et al.. SPRAY-DRIED CHITOSAN-METAL MICROPARTICLES FOR CIPROFLOXACIN ADSORPTION: KINETIC AND EQUILIBRIUM STUDIES. *Soft Matter*, 2011, 7 (16), pp.7304. 10.1039/c1sm05509g . hal-04101299

**HAL Id: hal-04101299**

**<https://hal.science/hal-04101299>**

Submitted on 19 May 2023

**HAL** is a multi-disciplinary open access archive for the deposit and dissemination of scientific research documents, whether they are published or not. The documents may come from teaching and research institutions in France or abroad, or from public or private research centers.

L'archive ouverte pluridisciplinaire **HAL**, est destinée au dépôt et à la diffusion de documents scientifiques de niveau recherche, publiés ou non, émanant des établissements d'enseignement et de recherche français ou étrangers, des laboratoires publics ou privés.

# SPRAY-DRIED CHITOSAN-METAL MICROPARTICLES FOR CIPROFLOXACIN ADSORPTION: KINETIC AND EQUILIBRIUM STUDIES

Franceline Reynaud<sup>1,2,3,4</sup>, Nicolas Tsapis<sup>1,2</sup>, Michel Deyme<sup>1,2</sup>, Tibiriça G.Vasconcelos<sup>5</sup>,  
Claire Gueutin<sup>1,2</sup>, Sílvia S. Guterres<sup>3</sup>, Adriana R. Pohlmann<sup>6</sup> and Elias Fattal<sup>1,2</sup>.

<sup>1</sup> Univ Paris-Sud, CNRS UMR 8612, 5 rue Jean-Baptiste Clément, Châtenay-Malabry, France.

<sup>2</sup> CNRS, UMR 8612, 5 rue Jean-Baptiste Clément, Châtenay-Malabry, France.

<sup>3</sup> Faculdade de Farmácia, Univ Federal Rio Grande do Sul, Av. Ipiranga, 2752, 90610-000, Porto Alegre, RS, Brazil.

<sup>4</sup> Faculdade de Farmácia, Univ Federal Rio de Janeiro, Ilha do Fundão, CCS bloco K, 21941-590, Rio de Janeiro, RJ, Brazil

<sup>5</sup> Departamento de Química, Univ Federal de Santa Maria, 97105-900, Santa Maria, RS, Brazil.

<sup>6</sup> Instituto de Química, Univ Federal Rio Grande do Sul, CP 15003, 91501-970, Porto Alegre, RS, Brazil.

Corresponding author:

Nicolas Tsapis, Univ Paris-Sud, CNRS UMR 8612, 5 rue Jean-Baptiste Clément, Châtenay-Malabry, France.

Email : [nicolas.tsapis@u-psud.fr](mailto:nicolas.tsapis@u-psud.fr)

Co-corresponding author:

Adriana R. Pohlmann, Instituto de Química, Univ Federal Rio Grande do Sul, CP 15003, 91501-970, Porto Alegre, RS, Brazil.

Email: [pohlmann@iq.ufrgs.br](mailto:pohlmann@iq.ufrgs.br)

## **Abstract**

Chitosan, a natural polysaccharide obtained from chitin deacetylation, complexes with metal ions by coordination with the free electrons pairs of amine groups. Based on this complexation mechanism, cross-linked chitosan-metal microparticles were prepared by spray drying using iron (II or III) or zinc ions and characterized in terms of size distribution and capacity to specifically adsorb ciprofloxacin. Chitosan-Zn(II) and chitosan-Fe(III) microparticles appear to adsorb more ciprofloxacin than plain chitosan or chitosan-Fe(II) microparticles. Adsorption isotherms for CH and CH-Fe(II) microparticles can be fitted by a single logarithm model (slope 1) with one ciprofloxacin per adsorption site, whereas for CH-Fe(II) and CH-Zn(II) microparticles isotherms are rather bilogarithmic with an initial slope of 2, suggesting that a single adsorption site can bind two molecules of ciprofloxacin. In addition, the pseudo second order kinetic model fits well experimental data, proving that adsorption is mediated by a chemical reaction. CH-Fe(II) and CH-Zn(II) appear very promising for drug elimination, either from hospital waste water or from the gastrointestinal tract to prevent the emergence of antibiotic resistance.

**Keywords:** spray-drying, chitosan, metal, ciprofloxacin, adsorption.

## 1. Introduction

Recently, the scientific community started to consider residual pharmaceuticals as potential pollutants and research about the behavior of these compounds and their metabolites has constantly grown<sup>1-4</sup>. It has been shown that concentrations of drugs/metabolites in hospital wastewater, sewage treatment plants (STPs), surface water or even in drinking water range from  $\text{ng.L}^{-1}$  to  $\mu\text{g.L}^{-1}$ <sup>5-7</sup>. In drinking water, although concentrations are lower than those administered therapeutically, chronic effects on humans when exposed are still unknown and drugs often present low or no biodegradability<sup>8-10</sup>.

Antibiotics<sup>11-12</sup> as well as resistant bacteria<sup>13</sup> have been found in environmental compartments. Indeed, the intestinal tract is the site where most antibiotic resistance develops<sup>14-15</sup>. In major cases, residual colonic antibiotics provided by orally administered or parenterally administered followed by intestinal secretion can give rise to the emergence of resistance to antibiotics by a process in which commensal resistant bacteria are first selected in the natural human or animal ecosystems. These bacteria can then transfer resistance mechanisms horizontally to pathogenic species either in the same host in whom the resistant commensals have emerged, or in another host after inter-individual transmission of the resistant commensals<sup>16-18</sup>. Another possibility is the rejection of the antibiotic itself in the ecosystem which can as well induce the selection of resistant bacteria but also induce other adverse effects behaving such as signaling molecules that may regulate the homeostasis of microbial communities<sup>17, 19-21</sup>. Moreover, common receptors have been identified in plants for a number of antibiotics affecting number of biological process such as chloroplast replication, transcription and translation, folate biosynthesis, fatty acid synthesis and sterol biosynthesis<sup>22</sup>.

Among all antibiotics, ciprofloxacin, a synthetic fluoroquinolone, is a broad-spectrum antibacterial agent for oral administration, used to treat various bacterial infections<sup>23</sup>. However, ciprofloxacin presents a low biodegradability even in the presence of sewage treatment plants in effluents<sup>24-25</sup>, and can still exert its deleterious effect on the environment<sup>26 27</sup>. Moreover, as it is the antibiotic reaches surface water<sup>8, 11</sup>. A study on the ecotoxicological effects of ciprofloxacin antibiotic in the aquatic environment demonstrated significant impact on the rate of algal biomass production and algal community structure<sup>28</sup>.

Investigations of technologies to treat effluents containing ciprofloxacin are therefore crucial. Advanced oxidation processes (AOPs) like ozone- and photo-based ones have demonstrated good potential<sup>29</sup> in transforming ciprofloxacin. Although these AOPs are

promising alternatives, they generate by-products with low biodegradability<sup>30</sup> and more research on the environmental characteristics of these compounds is needed. As an alternative to AOPs, we intend to develop a system that combines the ability of chitosan to bind metal ions with the natural complexation of antibiotics such as ciprofloxacin with the same metal ions. Chitosan-metal microparticles were therefore designed for ciprofloxacin removal.

The polyaminosaccharide chitosan is the deacetylated derivative of chitin, a naturally occurring polymer found in the shells of crustacean, the cuticles of insects and cell walls of some fungi<sup>31 32</sup>. Due to its biocompatibility, biodegradability, bioactivity and low toxicity, this biopolymer has been used for flocculation and coagulation in food processing, in heavy-metal ion recovery from wastewaters and in fabrication of structural matrices for food, cosmetic, biotechnological and biomedical applications<sup>33</sup>. Considering the extra electron pair of nitrogen, chitosan can form polymer-metal complexes with many metal cations<sup>34-35</sup> and is thus used as a metal-ion sorbent. Studies have shown that the metal ion is complexed with chitosan through the oxygen and the nitrogen of the aminosaccharide group<sup>34-37</sup>. Possible applications of the metal binding property are wastewater treatment for heavy metal and radio isotope removal with valuable metal recovery, and drinking water purification for reduction of unwanted metals<sup>38</sup>. Ciprofloxacin is able of forming strong complexes with multivalent metal ions. The stability of the complex formed is greatly dependent on the nature of the metal ion involved, and the environmental conditions. In the case of ciprofloxacin, the complex formation constant with iron ions is very high and the complex ciprofloxacin:metal stability declines in order: Fe(III)  $\approx$  Al(III) > Cu(II) > Fe(II)  $\approx$  Zn (II) > Mg(II) > Ca(II)<sup>39-41</sup>

In this paper, the efficiency of chitosan-metal microparticles to adsorb ciprofloxacin was evaluated as a function of the type of metal ions, the contact time and the concentration of ciprofloxacin. More important, we tried to give insight into the mechanism of adsorption by confronting experimental data for both isotherm and kinetics with theoretical models.

## *2. Materials and methods*

### *2.1 Materials*

Chitosan (CH), zinc acetate dehydrate, and ciprofloxacin were obtained from Fluka (Switzerland). Glutaraldehyde and sodium acetate were provided by VWR (France). Iron (II) chloride was from Acros Organic (Belgium). Hydroxyethylpiperazine-ethanesulfonic

acid (HEPES), 1-(2-pyridylazo)-2-naphthol (PAN), ammonia buffer (pH 10) for complexometry, hydroxylamine hydrochloride, 1,10-phenantroline and iron(III) nitrate were obtained from Sigma-Aldrich (France). HPLC grade solvents were supplied by Carlo Erba (Italy).

## *2.2 Preparation of Chitosan-metal microparticles*

Chitosan-metal (CH-metal) complexes were prepared according to a modification of a procedure previously described<sup>34</sup>. Briefly, solutions were obtained by dissolving chitosan (1% w/v) in a metal ion aqueous solution ( $\text{FeCl}_2$  0.1M;  $\text{Fe}(\text{NO}_3)_3$  0.1M and  $\text{Zn}(\text{CH}_3\text{COO})_2$  0.1M). They were maintained upon magnetic stirring for 12 h at room temperature (20°C) to yield CH-metal complexation. The metal complexation capacity of chitosan is strongly affected by the pH of the solution. For each of these metals, there is an optimal complexation pH which is rather acidic in order to reduce the formation  $-\text{NH}^{+3}$  groups unfavorable for complexation. Therefore, in our conditions, the pH was fixed at 5 as a compromise that permits to compare the different chitosan-metal complexes prepared under the same conditions.

CH-metal microparticles were then prepared by spray-drying. The chitosan-metal complex solutions prepared above (200 mL) were spray-dried using a Buchi<sup>®</sup> Mini Spray Dryer, type B191 (Switzerland) with a standard 0.7 mm nozzle at a feed rate of 5 ml.min<sup>-1</sup>. The atomizing air flow rate was 600 L.h<sup>-1</sup> and the aspiration of 100%. The inlet temperature was controlled at 150°C and the outlet temperature varied between 80-100°C.

## *2.3 Microparticles cross-linking*

After spray-drying, CH-metal microparticles were suspended into a 0.025M glutaraldehyde (GLA) solution to obtain a 1:1 molar ratio with chitosan (mol GLA: mol  $\text{NH}_2$ ). Non-cross-linked microparticles (1 g) were suspended under magnetic stirring for 4 h in a glutaraldehyde solution (25% in acetone, 100 mL). Microparticles were then filtered and washed with ethanol-water (2:1, v/v) solutions to remove the excess of metal ions and glutaraldehyde, and finally vacuum-dried for at least 24 h.

## *2.4 Microparticles size distribution*

A Mastersizer 2000 granulometer equipped with a Scirocco dry disperser (Malvern Instruments, France) was used to determine CH-metal microparticle size distribution. Average particle size was expressed as the volume mean diameter ( $D_{4,3}$ ). Polydispersity was given by the span index, which was calculated according to Eq. (1):

$$Span = (D_{0.9} - D_{0.1}) / D_{0.5} \quad (1)$$

where  $D_{0.9}$ ,  $D_{0.5}$  and  $D_{0.1}$  are the particle diameters determined respectively at the 90<sup>th</sup>, 50<sup>th</sup> and 10<sup>th</sup> percentile of undersized particles.

## 2.5 Scanning Electron Microscopy (SEM)

Microparticle morphology was evaluated by scanning electron microscopy using a LEO 9530, Gemini (France) at an accelerating voltage of 3kV. Prior to observation, samples were mounted on metal stubs, using carbon-conductive double-sided adhesive tape, and coated with a 4 nm platinum/palladium layer under vacuum (Cressington 208 HR, Eloise, France).

## 2.6 Degree of deacetylation

The degree of deacetylation of the chitosan and CH-metal microparticles was determined by infrared spectrometry. A thin film of microparticles was used to record an infrared spectrum using a Spectrum One FT-IR and a Diamond ATR accessory (Perkin Elmer). The absorbance at  $1.655 \text{ cm}^{-1}$  for amide-I and at  $3.450 \text{ cm}^{-1}$  for OH groups in chitosan were determined. The degree of deacetylation (DDA) was then calculated using Eq. (2) <sup>42</sup>

$$DDA(\%) = [1 - (A_{1.655} / A_{3.450}) / 1.33] \times 100 \quad (2)$$

where factor 1.33 represents the  $A_{1.655}/A_{3.450}$  ratio for fully N-acetylated chitosan.

## 2.7 Metal determination

### 2.7.1 Iron determination

The quantity of iron associated to cross-linked CH-iron microparticles was determined by a spectrophotometric method using 1,10-phenantroline for colorimetry as described<sup>43</sup>. Cross-linked CH-Fe(II) and CH-Fe(III) microparticles were first submitted to acid hydrolysis (100 mg/ 5 mL HCl:HNO<sub>3</sub> 1:1 v:v). Iron Standards solutions containing different concentrations of iron (0.1-2.5 µg.mL<sup>-1</sup>) were prepared. Briefly, 1 µl of samples containing iron ions, 2 mL of hydroxylamine hydrochloride solution (1 g.mL<sup>-1</sup>) and 5 mL acetate buffer solution were placed in volumetric flasks of 10 mL. 2 mL of 1,10-phenantroline (1g.L<sup>-1</sup>) stock solution were added and the volume was adjusted to 10 mL with water. After 20 min, an orange-red complex was formed. Absorbances were measured at 510 nm against free iron solution using a UV-2101PC spectrophotometer (Shimadzu, Japan).

### 2.7.2 Zinc determination

The quantity of Zn(II) associated to chitosan was determined according to a modification of procedure described in the literature<sup>18, 44</sup>. Briefly, cross-linked CH-Zn(II) microparticles were submitted to acid hydrolysis (100 mg/ 5 mL HCL:HNO<sub>3</sub> 1:1 v:v). Standard zinc solutions containing known concentrations of zinc ions (25 - 300 µg.mL<sup>-1</sup>) were prepared. 1µl of samples containing zinc ions and 1 mL of ammonia buffer solution (pH 10) were placed into a volumetric flask. 3mL of ethanolic PAN stock solution (5.0x10<sup>-4</sup>M) were added and the volume was adjusted to 10mL with ethanol. The sample was then shaken and left to stand in a thermostated water bath for 10 min. at 40°C to allow complete formation of the PAN-Zn complex. The amount of zinc was determined by measuring the absorbance at 550nm against free zinc solution (UV-2101PC Shimadzu, Japan).

### 2.8 Ciprofloxacin adsorption by chitosan-metal microparticles

Adsorption experiments were carried out by a batch technique. CH or CH-metal microparticles (CH, CH-Fe(II), CH-Fe(III) or CH-Zn(II)) were incubated at 1mg/mL in HEPES buffer (pH = 6.5) containing ciprofloxacin at various concentrations (25, 50, 100, 200, 300 and 400 µg.mL<sup>-1</sup>). The flasks were sealed to prevent change in volume of the solution during the experiments and they were submitted to a gentle tangential stirring, at 37±2°C for 300 min. Samples were taken at pre-determined time intervals (30, 60, 90, 120, 180, 240 and 300 min.), centrifuged at 4000 rpm for 3 min and the supernatant was analyzed for the remaining ciprofloxacin concentration by high performance liquid

chromatography (HPLC) following method described in section 2.8.1. All experiments were carried out in duplicates.

The uptake of ciprofloxacin by unit mass of adsorbent ( $q$ ) at any time was determined from Eq. (3):

$$q = \frac{C_0 - C}{\alpha} \quad (3)$$

where  $C_0$  and  $C$  are the initial and remaining unadsorbed ciprofloxacin concentration ( $\mu\text{g.mL}^{-1}$ ) in solution at any time and  $\alpha$  is the microparticle concentration ( $\text{mg.mL}^{-1}$ ).

### 2.8.1 Chromatographic system and conditions

The HPLC system consisted of a Waters 510 pump (with an on-line degasser), a Waters 717plus autosampler, a Waters 470 fluorescence detector and column heater. The wavelength of excitation was set at 280 nm and the wavelength of emission at 460 nm, Chromatographic separations were performed in 10 min (flow rate  $1\text{mL.min}^{-1}$ ), at  $40^\circ\text{C}$  using a C18 Symmetry<sup>®</sup> column ( $5\ \mu\text{m}$ ,  $150 \times 4.6\ \text{mm}$ ; Waters, France). The mobile phase consisted of a mixture of acetonitrile and phosphate buffer solution 10 mM (15:85 v/v), acidified at pH 3 with orthophosphoric acid. Data acquisition and analysis was performed using the Azur<sup>®</sup> software.

## 2.9 Modeling of sorption equilibrium and kinetics of ciprofloxacin

### 2.9.1 Modeling of sorption equilibrium

Equilibrium data, commonly known as adsorption isotherms, are basic requirements for the design of adsorption systems used for removal of organic compounds from solutions. The Langmuir and Freundlich equations are the most frequently used for data interpretation. The mathematical description of Langmuir model follows Eq. (4):

$$q = \frac{K_L C_{eq} M_{max}}{(1 + K_L C_{eq})} \quad (4)$$

where  $C_{eq}$  is the unadsorbed ciprofloxacin concentrations, and  $q$  the uptake of ciprofloxacin by unit mass of adsorbent given by Eq. 3.  $M_{max}$  represents a practical limiting

adsorption capacity when the surface is fully covered with antibiotic and  $K_L$  is a constant related to the affinity of the binding sites.  $K_L$  and  $M_{max}$  can be determined from the linear plot of  $1/q$  versus  $1/C_{eq}$ . The Langmuir model assumption is that one adsorption site can bind one molecule.

The mathematical description of Freundlich model follows Eq. (5):

$$q = K_F C_{eq}^\beta \quad (5)$$

where  $K_F$  and  $\beta$  are the Freundlich constants related to the adsorption capacity and adsorption intensity of the sorbent, respectively. This model can be linearized in logarithmic form and Freundlich constants can be determined.

### 2.9.2 Modeling of adsorption kinetics of ciprofloxacin

The adsorption kinetics of ciprofloxacin may be described by pseudo-first-order<sup>45</sup> and pseudo-second-order<sup>46</sup> kinetic models. The pseudo-first-order model is based on sorbent capacity and considers that the rate of occupation of adsorption sites is proportional to the number of unoccupied sites. The pseudo-first-order equation follows in Eq. (6):

$$\text{Log}(q_{eq} - q) = \log q_{eq} - \frac{K_{1,ad}}{2.303} t \quad (6)$$

where  $q_{eq}$  and  $q$  refer to the amount of ciprofloxacin adsorbed (both in  $\mu\text{g.mg}^{-1}$ ) at the equilibrium time and time  $t$  (min), respectively.  $K_{1,ad}$  ( $\text{min}^{-1}$ ) is the equilibrium rate constant of pseudo-first-order sorption. A straight line of  $\text{Log}(q_{eq} - q)$  versus  $t$  suggests the applicability of this kinetic model.

The pseudo-second-order equation is also based on the adsorption capacity of the solid phase and expressed as follows in Eq. (7):

$$\frac{t}{q} = \frac{1}{K_{2,ad} q_{eq}^2} + \frac{1}{q_{eq}} t \quad (7)$$

where  $K_{2,ad}$  ( $\text{mg} \cdot \mu\text{g}^{-1} \cdot \text{min}^{-1}$ ) is the rate constant for pseudo-second-order adsorption kinetics. If second-order kinetics is applicable, the plot of  $t/q$  versus  $t$  should give a linear relationship, from which  $q_{eq}$  and  $K_{2,ad}$  can be determined from the slope and the intercept of the plot respectively.

### 3 Results and discussion

#### 3.1 Characteristics of chitosan and chitosan-metal microparticles

When suspended in aqueous solution, non-cross-linked chitosan microparticles do not maintain the form of spheres, especially in an acidic environment: they swell and dissolve<sup>47</sup>. The swelling and dissolution behavior of the microparticles depend on the degree of deacetylation of chitosan<sup>42</sup>. In order to prepare insoluble/stable chitosan microparticles suited for drug adsorption, cross-linking agents such as glutaraldehyde, are generally used<sup>32</sup>. The morphology of the chitosan and CH-metal microparticles (cross-linked and non-cross-linked) was examined by scanning electron microscopy (SEM) (Figure 1). Microparticles are polydisperse in size and present spherical collapsed shapes, independently of cross-linking. The collapse shape is characteristic of buckled shells due to the quick drying process<sup>48,49,50</sup>. Cross-linking does not influence surface roughness. Surface roughness of CH microparticles is more important than for CH-metal microparticles, probably due to differences in mechanical properties of CH and CH-metal solutions as they dry. Characteristics of CH and CH-metal microparticles, either cross-linked or not are listed in Table 1. Particle size distribution of non-cross-linked microparticles is rather polydisperse with span values between 2 and 68. The polydispersity may arise from two phenomena: first, the viscosity of the solutions may lead to an inhomogeneous droplet distribution in the spray-dryer, second, surface properties may induce particle sticking. Non-cross-linked CH-Zn(II) microparticles present the lower span. Microparticle size distribution is strongly influenced by the cross-linking process. Indeed, after cross-linking, microparticle size distribution becomes narrower except for CH-Fe(II) which remains polydisperse and for CH-Zn(II) which was already narrow. Cross-linking may modify the chemistry of particles surface and therefore their tendency to aggregation.

To assess the efficacy of metal complexation and of cross-linking, the degree of deacetylation (DDA) of CH and CH-metal microparticles was determined by an infrared technique. The FT-IR spectra of CH and CH-metal microparticles (crosslinked and non-

cross-linked) are given in Figure 2. The bands at 900 and 1050  $\text{cm}^{-1}$ , characteristic of saccharide structure, are present in all spectra. The bands corresponding to C–H stretching are observed at 2864  $\text{cm}^{-1}$  and 2932  $\text{cm}^{-1}$  and free hydroxyl at 3290  $\text{cm}^{-1}$ . The ratio of absorbance of amide I at 1655  $\text{cm}^{-1}$  on that of hydroxyl group at 3450  $\text{cm}^{-1}$  in the CH-metal microparticles is related to the degree of polymer deacetylation by Eq. 2. The DDA of the microparticles decreases from 75% to 19-25% after complexation with metal ions for non-cross-linked microparticles, indicating that complexation of metal ions with chitosan polymer takes place by reaction with amine groups of chitosan (Table 1). For all cross-linked samples the presence of a weak band at 1560  $\text{cm}^{-1}$  corresponding to imine bond (C=N) confirms the reaction between the aldehyde (CHO) and the  $\text{NH}_2$  sites of chitosan. **This reaction may decrease the cytotoxicity as shown previously<sup>51</sup>. Furthermore,** there is no evidence of a carbonyl band near 1720  $\text{cm}^{-1}$  indicating that all unreacted glutaraldehyde is removed after the washing procedure. In addition, the DDA decreases after the cross-linking process.

### 3.2 Metal determination

Before cross-linking, CH-Fe(II) and CH-Fe(III) microparticles contain 66  $\text{mg.g}^{-1}$  and 191  $\text{mg.g}^{-1}$  of iron respectively and Ch-Zn microparticles contain 114  $\text{mg.g}^{-1}$  of zinc. It correspond to 17.6, 53 and 28.8% of the initial metal. After cross-linking, the metal concentration decreases: cross-linked chitosan CH-Fe(II) microparticles contain 45  $\text{mg.g}^{-1}$  iron whereas cross-linked chitosan CH-Fe(III) microparticle contain 130  $\text{mg.g}^{-1}$  iron, corresponding respectively to 12% and 36% of initial Fe(II) and Fe(III). Cross-linked CH-Zn(II) showed 87  $\text{mg.g}^{-1}$ , corresponding to 22% of Zn(II) added in the reaction. The decrease of the metal associated to microparticles after cross-linking indicates that the amine groups implicated in the cross-linking are also implicated in the association with metal ions. This result confirms the decrease of the DDA observed after cross-linking.

### 3.3 Ciprofloxacin adsorption by chitosan-metal microparticles

#### 3.3.1 Uptake capacity of the chitosan-metal microparticles

The effect of contact time on ciprofloxacin adsorption was analyzed by plotting uptake capacity ( $q$ ) versus time, for 25, 50, 100, 200, 300 and 400  $\mu\text{g.mL}^{-1}$  initial ciprofloxacin concentrations, at constant temperature (37°C). Initially, a large number of

adsorption sites are free and ciprofloxacin adsorption occurs quickly. The adsorption equilibrium of ciprofloxacin onto CH and CH-Fe(II) microparticles is reached after 30 min only (Fig. 3 (1) and (2)). Almost no significant improvement is observed for longer contact times. For these microparticles, the initial ciprofloxacin concentration does not influence the equilibrium time.

By contrast, the adsorption equilibrium of ciprofloxacin onto CH-Fe(III) and CH-Zn(II) microparticles seems to be influenced by the initial ciprofloxacin concentration. For low ciprofloxacin concentrations (25; 50 and 100  $\mu\text{g.mL}^{-1}$ ) the equilibrium state was reached around 120 min and 180 min for CH-Fe(III) and CH-Zn(II), respectively [Fig. 3 (3) and (4)]. For higher ciprofloxacin concentrations (200; 300 and 400  $\mu\text{g.mL}^{-1}$ ) the equilibrium state was achieved at 300 min. No significant adsorption improvement can be observed for longer contact times (8 and 24h, data not shown). For example for an initial ciprofloxacin concentration of 400  $\mu\text{g.mL}^{-1}$ , one milligram of CH-Fe(III) microparticles can adsorb up to 305, 320 and 304  $\mu\text{g}$  after 5, 8 and 24h, respectively. One milligram of CH-Zn(II) microparticles can adsorb up to 330, 325 and 328  $\mu\text{g}$  ciprofloxacin after 5, 8 and 24h, respectively.

Indeed the initial ciprofloxacin concentration can influence the adsorption process. To verify this influence, the effect of initial ciprofloxacin concentration was studied between 25 to 400  $\mu\text{g.mL}^{-1}$ , for all microparticles and the uptake capacity ( $q_{300}$ ) and adsorption yields at 300min are presented in Table 2. The equilibrium ciprofloxacin uptake was significantly enhanced as the initial concentration of ciprofloxacin increased from 25 to 400  $\mu\text{g.mL}^{-1}$ . For CH microparticles, the uptake capacity increases from 2.8 to 32.9  $\mu\text{g.mg}^{-1}$  whereas for CH-Fe(II) it increases from 8.7 to 105.7  $\mu\text{g.mg}^{-1}$ . The presence of the metal strongly enhances microparticle adsorption capacity. This increase is even more obvious for CH-Fe(III) and CH-Zn(II) for which the uptake capacity increases from 20.5 to 305.3  $\mu\text{g.mg}^{-1}$  and from 15.5 to 302  $\mu\text{g.mg}^{-1}$ , respectively. The equilibrium uptakes and adsorption yields of CH-Fe(III) and CH-Zn(II) were much higher than those of CH-Fe(II) and CH microparticles (Figure 4). This variation in the sorption capacity between the sorbents is related to the amount of metal ions associated to microparticles: the higher the metal associated to chitosan, the higher the ciprofloxacin adsorption. However, although there is less Zn(II) than Fe(III) associated to CH, the affinity of ciprofloxacin with Zn(II) is higher, therefore leading to a better adsorption capacity for CH-Zn(II) microparticles.

### 3.3.2 Adsorption isotherms

In order to optimize the design of an adsorption system it is important to establish the most appropriate model for the equilibrium isotherms. These isotherms were determined by incubating microparticles ( $1 \text{ mg.mL}^{-1}$ ) in a HEPES buffer solution containing ciprofloxacin at various concentration ( $25 - 400 \text{ }\mu\text{g.mL}^{-1}$ ) and plotting  $\log(q_{eq})$  (adsorption capacity at time 300 min = at equilibrium) versus  $\log(C_{eq})$  (equilibrium concentration of ciprofloxacin) (Figure 5). Neither the Langmuir model nor the Freundlich one fit experimental data. For CH and CH-Fe(II) microparticles, experimental data can be fitted by a straight line whose slope is equal to one. Saturation seems to start for CH-Fe(II) around  $100 \text{ }\mu\text{g.mg}^{-1}$ . For CH-Fe(III) and CH-Zn(II) microparticles, the plot is bilogarithmic with a  $n=2$  initial slope, followed by a plateau indicating saturation around  $200 \text{ }\mu\text{g.mg}^{-1}$ . These data suggest that the adsorption site of CH or CH-Fe(II) can bind a single ciprofloxacin molecule whereas the adsorption site of CH-Fe(III) and CH-Zn(II) microparticles can bind two ciprofloxacin molecules.

### 3.3.3 Adsorption kinetics

Adsorption kinetics has been proposed to elucidate the origin of adsorption. The mechanism of adsorption depends on the physical and chemical characteristics of the sorbent as well as on the mass transport process. To investigate whether the mechanism of ciprofloxacin adsorption on CH-metal microparticles occurs by mass transfer (physisorption) or chemical reaction (chemisorption), two kinetic models were examined: the pseudo-first-order model<sup>45</sup> and the pseudo-second-order model<sup>46</sup>. The first-order rate constant ( $K_{1,ad}$ ) and  $q_{300,1,calc}$  values are presented with the correlation coefficients in Table 4. The  $K_{1,ad}$  values do not seem to be influenced by ciprofloxacin initial concentration or the particles used. In addition, theoretical  $q_{300}$  values obtained from the first-order kinetic model do not give reasonable values. Using Eq (7),  $t/q$  was plotted against  $t$ , and second-order adsorption rate constant ( $K_{2,ad}$ ) and equilibrium uptake values ( $q_{300,2,calc}$ ) were determined from the slope and the intercept of plots (data not shown). Values of  $K_{2,ad}$  and  $q_{300,2,calc}$  and of correlation coefficients are presented in Table 4. The correlation coefficient of pseudo-second-order equation is always higher than that of pseudo-first-order. In addition the theoretical  $q_{300}$  value calculated from the pseudo-second-order model is closer to the experimental  $q_{300}$  value than the one obtained from the pseudo-first-order model.

The pseudo-second-order adsorption mechanism is predominant for the adsorption of ciprofloxacin on CH-metal microparticles indicating that the adsorption process is mainly due to chemisorption. The chemisorption of ciprofloxacin on CH-metal microparticles may arise from the presence of the carboxylic group and the keto oxygen group as observed by others<sup>39</sup>. For Fe(III) and Zn(II) that are hexavalent one CH-Metal complex may bind two ciprofloxacin and for Fe(II) that is tetravalent only one ciprofloxacin may be bound to CH-Fe(II) in agreement with the slope of the adsorption isotherms. Additional structural studies using techniques such as X-ray absorption spectroscopy should be performed to determine the exact organization of the CH-metal-quinolone complexes<sup>52</sup>.

## Conclusion

Chitosan-metal microparticles were prepared by a conventional spray-drying method followed by crosslinking using glutaraldehyde. Their capacity to adsorb ciprofloxacin, an antibiotic often responsible of the emergence of antibiotic resistance, was investigated as a function of contact time and initial drug concentration. Results show that the adsorption isotherms are fitted either by monologarithmic model for CH and CH-Fe(II) microparticles with one ciprofloxacin per adsorption site, or by a bilogarithmic model with a initial slope of two for CH-Fe(III) and CH-Zn(II) with two ciprofloxacin per adsorption site. In addition, the adsorption kinetics are well described by a pseudo-second-order kinetic model, indicating that the adsorption mechanism is controlled by chemisorption. CH-Fe(III) and CH-Zn(II) microparticles present a high adsorption capacity of ciprofloxacin, revealing that these particles could be employed as promising adsorbent for ciprofloxacin removal either from hospital waste water or from the gastrointestinal tract to prevent the emergence of antibiotic resistance.

**Acknowledgements**F. Reynaud acknowledges financial support from CAPES/COFECUB. Authors would like to thank M.F. Trichet (ICMPE, Thiais) for access to the SEM facility and CNRS, Univ Paris-Sud and CNPq-MCT/Brazil for funding.

## References

1. T. Erbe, K. Kummerer, S. Gartiser and L. Brinker, *Rofo*, 1998, **169**, 420-423.
2. J. Oppel, G. Broll, D. Loffler, M. Meller, J. Rombke and T. Ternes, *Sci Total Environ*, 2004, **328**, 265-273.
3. K. Kümmerer, *Pharmaceuticals in the Environment: Sources, Fate Effects and Risks*, Springer, Berlin, Heidelberg, 2008.
4. M. Brinke, S. Hoss, G. Fink, T. A. Ternes, P. Heiningner and W. Traunspurger, *Aquat Toxicol*, 2010, **99**, 126-137.
5. A. F. Martins, T. G. Vasconcelos, D. M. Henriques, C. D. Frank, A. König and K. Kummerer, *Clean-Soil Air Water*, 2008, **36**, 264-269.
6. A. Garcia-Ac, P. A. Segura, L. Viglino, A. Furtos, C. Gagnon, M. Prevost and S. Sauve, *Journal of Chromatography A*, 2009, **1216**, 8518-8527.
7. M. Gros, M. Petrovic, A. Ginebreda and D. Barcelo, *Environment International*, 2010, **36**, 15-26.
8. B. Halling-Sorensen, H. C. H. Lutzhoft, H. R. Andersen and F. Ingerslev, *Journal of Antimicrobial Chemotherapy*, 2000, **46**, 53-58.
9. Y. Kim, K. Choi, J. Y. Jung, S. Park, P. G. Kim and J. Park, *Environment International*, 2007, **33**, 370-375.
10. C. Fernandez, M. Gonzalez-Doncel, J. Pro, G. Carbonell and J. V. Tarazona, *Science of the Total Environment*, 2010, **408**, 543-551.
11. D. W. Kolpin, E. T. Furlong, M. T. Meyer, E. M. Thurman, S. D. Zaugg, L. B. Barber and H. T. Buxton, *Environmental Science & Technology*, 2002, **36**, 1202-1211.
12. E. Zuccato, S. Castiglioni, R. Bagnati, M. Melis and R. Fanelli, *Journal of Hazardous Materials*, 2010, **179**, 1042-1048.
13. J. L. Caplin, G. W. Hanlon and H. D. Taylor, *Environ Microbiol*, 2008, **10**, 885-892.
14. M. P. Nikolich, G. Hong, N. B. Shoemaker and A. A. Salyers, *Appl Environ Microbiol*, 1994, **60**, 3255-3260.
15. T. F. O'Brien, D. G. Ross, M. A. Guzman, A. A. Medeiros, R. W. Hedges and D. Botstein, *Antimicrob Agents Chemother*, 1980, **17**, 537-543.
16. H. G. de Vries-Hospers, R. H. Tonk and D. van der Waaij, *Scand J Infect Dis*, 1991, **23**, 625-633.
17. D. van der Waaij and C. E. Nord, *International Journal of Antimicrobial Agents*, 2000, **16**, 191-197.
18. M. Khoder, N. Tsapis, V. Domergue-Dupont, C. Gueutin and E. Fattal, *Eur J Pharm Sci*, 2010, **41**, 281-288.
19. J. F. Linares, I. Gustafsson, F. Baquero and J. L. Martinez, *P Natl Acad Sci USA*, 2006, **103**, 19484-19489.
20. A. Fajardo and J. L. Martinez, *Curr Opin Microbiol*, 2008, **11**, 161-167.
21. A. Fajardo, N. Martinez-Martin, M. Mercadillo, J. C. Galan, B. Ghysels, S. Matthijs, P. Cornelis, L. Wiehlmann, B. Tummler, F. Baquero and J. L. Martinez, *Plos One*, 2008, **3**, -.
22. E. G. C. Brain, K. Rezai, F. Lokiec, M. Gutierrez and S. Urien, *Brit J Clin Pharmacol*, 2008, **65**, 607-610.
23. S. K. Upadhyay, P. Kumar and V. Arora, *J Struct Chem+*, 2006, **47**, 1078-1083.
24. R. Andreozzi, M. Raffaele and P. Nicklas, *Chemosphere*, 2003, **50**, 1319-1330.
25. S. Castiglioni, R. Bagnati, R. Fanelli, F. Pomati, D. Calamari and E. Zuccato, *Environmental Science & Technology*, 2006, **40**, 357-363.
26. A. Al-Ahmad, F. D. Daschner and K. Kummerer, *Arch Environ Contam Toxicol*, 1999, **37**, 158-163.
27. K. Kummerer, A. al-Ahmad and V. Mersch-Sundermann, *Chemosphere*, 2000, **40**, 701-710.
28. B. A. Wilson, V. H. Smith, F. Denoyelles and C. K. Larive, *Environmental Science & Technology*, 2003, **37**, 1713-1719.
29. T. G. Vasconcelos, D. M. Henriques, A. König, A. F. Martins and K. Kummerer, *Chemosphere*, 2009, **76**, 487-493.
30. T. G. Vasconcelos, K. Kummerer, D. M. Henriques and A. F. Martins, *J Hazard Mater*, 2009, **169**, 1154-1158.
31. C. Burger, D. Valcarenghi, S. Sandri and C. A. Rodrigues, *Int J Pharmaceut*, 2001, **223**, 29-33.
32. P. He, S. S. Davis and L. Illum, *Int J Pharmaceut*, 1999, **187**, 53-65.
33. S. A. Agnihotri and T. M. Aminabhavi, *J Control Release*, 2004, **96**, 245-259.
34. C. A. Rodrigues, F. Reynaud, E. Stadler and V. Drago, *J Liq Chromatogr R T*, 1999, **22**, 761-769.
35. X. H. Wang, Y. M. Du, L. H. Fan, H. Liu and Y. Hu, *Polym Bull*, 2005, **55**, 105-113.
36. S. C. Bhatia and N. Ravi, *Biomacromolecules*, 2000, **1**, 413-417.
37. A. C. Zimmermann, A. Mecabo, T. Fagundes and C. A. Rodrigues, *Journal of Hazardous Materials*, 2010, **179**, 192-196.
38. I. M. N. Vold, K. M. Varum, E. Guibal and O. Smidsrod, *Carbohydr Polym*, 2003, **54**, 471-477.

39. I. Turel, *Coordin Chem Rev*, 2002, **232**, 27-47.
40. V. Kmetec, F. Kozjek and M. Veber, *Int J Pharmaceut*, 1999, **176**, 225-230.
41. H. H. M. Ma, F. C. K. Chiu and R. C. Li, *Pharmaceut Res*, 1997, **14**, 366-370.
42. K. C. Gupta and F. H. Jabrail, *Carbohydr Polym*, 2006, **66**, 43-54.
43. *Standard Methods for the Examination of Water and Wastewater*, 19th edn., APHA-AWWA-WEF American Public Health Association, 1995.
44. M. Khoder, N. Tsapis, H. Huguet, M. Besnard, C. Gueutin and E. Fattal, *Int J Pharmaceut*, 2009, **379**, 251-259.
45. Y. Zhang, M. Yang and X. Huang, *Chemosphere*, 2003, **51**, 945-952.
46. Y. S. Ho and G. McKay, *Process Biochem*, 1999, **34**, 451-465.
47. I. Genta, M. Costantini, A. Asti, B. Conti and L. Montanari, *Carbohydr Polym*, 1998, **36**, 81-88.
48. N. Tsapis, D. Bennett, B. Jackson, D. A. Weitz and D. A. Edwards, *P Natl Acad Sci USA*, 2002, **99**, 12001-12005.
49. N. Tsapis, E. R. Dufresne, S. S. Sinha, C. S. Riera, J. W. Hutchinson, L. Mahadevan and D. A. Weitz, *Phys Rev Lett*, 2005, **94**, -.
50. R. Vehring, W. R. Foss and D. Lechuga-Ballesteros, *J Aerosol Sci*, 2007, **38**, 728-746.
51. E. D. Costa, M. M. Pereira and H. S. Mansur, *J Mater Sci-Mater M*, 2009, **20**, 553-561.
52. M. T. Klepka, N. Nedelko, J. M. Greneche, K. Lawniczak-Jablonska, I. N. Demchenko, A. Slawska-Waniewska, C. A. Rodrigues, A. Debrassi and C. Bordini, *Biomacromolecules*, 2008, **9**, 1586-1594.

Table 1

Physiochemical characteristics of non-cross-linked and cross-linked chitosan and CH-metal microparticles

Microparticle	Non-cross-linked						Cross-linked					
	D <sub>0.1</sub>	D <sub>0.5</sub>	D <sub>0.9</sub>	D <sub>4,3</sub>	Span	DDA (%)	D <sub>0.1</sub>	D <sub>0.5</sub>	D <sub>0.9</sub>	D <sub>4,3</sub>	Span	DDA (%)
CH	0.73 ±0.01	2.66 ±0.02	183.71 ±12.93	36.1 ±1.61	68.7 ±5.38	75	0.74 ±0.01	2.88 ±0.08	8.68 ±1.29	27.47 ±4.83	2.7 ±0.37	26
CH-Fe(II)	2.69 ±0.02	9.85 ±0.34	185.46 ±8.65	54.84 ±2.05	18.5 ±0.34	23	1.59 ±0.01	4.34 ±0.01	151.64 ±4.60	36.71 ±0.39	34.5 ±1.03	22
CH-Fe(III)	1.95 ±0.13	6.02 ±0.36	167.72 ±20.98	42.96 ±4.21	27.4 ±2.10	19	1.47 ±0.01	4.63 ±0.01	30.56 ±2.46	29.51 ±0.54	6.2 ±0.53	14
CH-Zn(II)	0.71 ±0.01	3.85 ±0.04	9.68 ±0.33	20.88 ±1.59	2.3 ±0.07	25	1.12 ±0.02	4.58 ±0.10	12.50 ±2.07	20.12 ±2.07	2.4 ±0.05	13

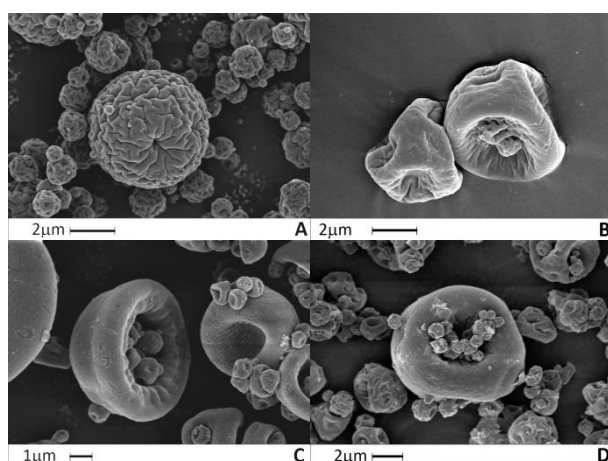


Figure 1: SEM figures of chitosan and CH-metal microparticles obtained by spray drying from aqueous solutions followed by cross-linking: (A) CH; (B) CH-Fe(II); (C) CH-Fe(III); (D) CH-Zn(II).

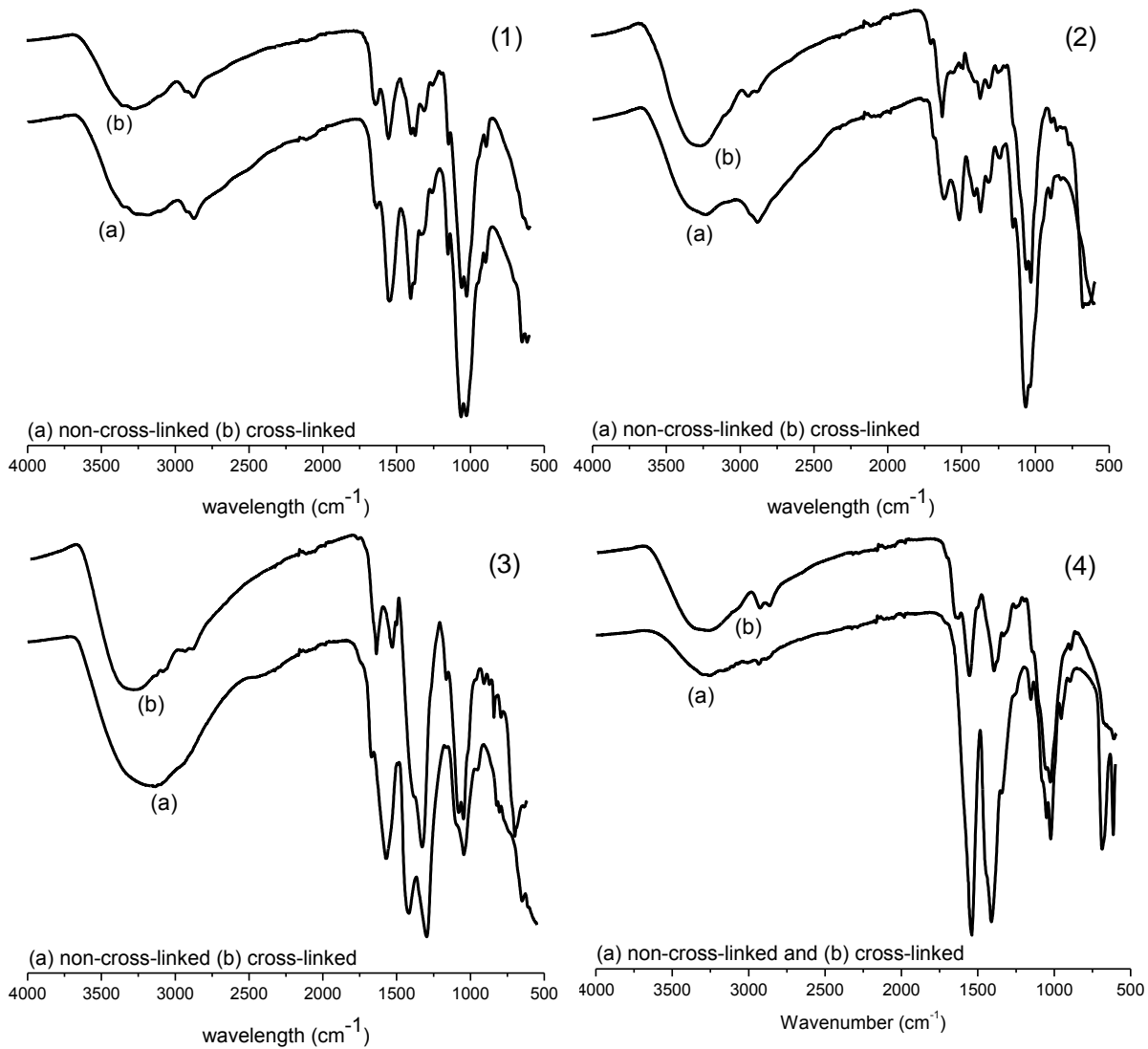


Figure 2: FT-IR spectrum of CH (1), CH-Fe(II) (2), CH-Fe(III) (3) and CH-Zn(II) (4) microparticles; (a) non-cross-linked and (b) cross-linked, for determining the degree of deacetylation using transmittance ratio of amide-I ( $1.655 \text{ cm}^{-1}$ ) and hydroxyl group ( $3.450 \text{ cm}^{-1}$ ).

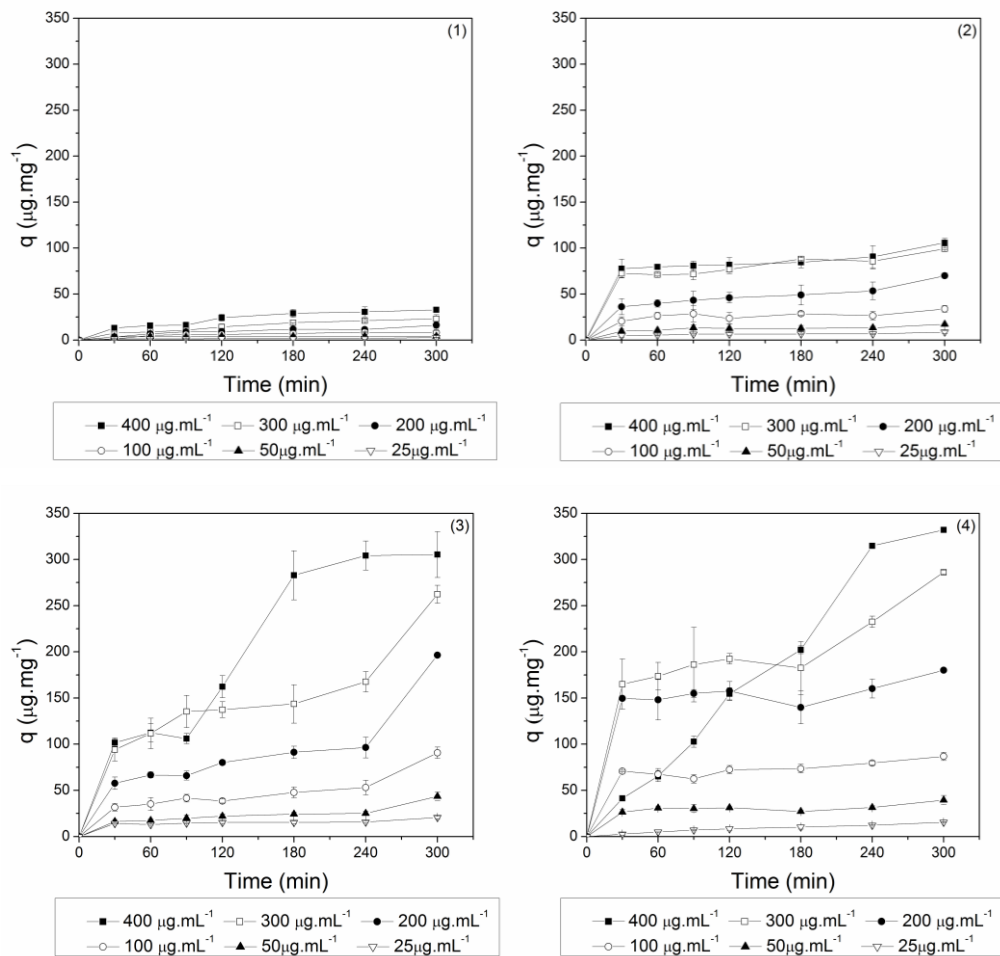


Figure 3: Effect of contact time and initial ciprofloxacin concentrations (25 – 400  $\mu\text{g.mL}^{-1}$ ) on ciprofloxacin adsorption on CH (1), CH-Fe(II) (2), CH-Fe(III) (3) and CH-Zn(II) (4) microparticles, in HEPES buffer (pH = 6.8, at 37°C).

Table 2: Comparison of the equilibrium uptake and adsorption yields of ciprofloxacin at different initial concentration to the CH, CH-Fe(II), CH-Fe(III) and CH-Zn(II) microparticles.

Ciprofloxacin ( $\mu\text{g.mL}^{-1}$ )	CH		CH-Fe(II)		CH-Fe(III)		CH-Zn(II)	
	$q_{300}$ ( $\mu\text{g.mg}^{-1}$ )	Adsorption (%)						
25	2.8±0.13	11.2	8.7±1.75	34.8	20.5±1.22	82.0	15.5±0.36	62.0
50	4.1±1.00	8.2	17.2±0.47	34.4	43.4±4.68	86.8	39.4±5.10	78.8
100	8.2±2.17	8.2	33.8±3.67	33.80	90.6±6.19	96.6	86,7±4,58	86.7
200	16.1±3.33	8.1	69.9±2.78	35.0	186.5±1.23	93.2	180.1±1.21	90.1
300	23.1±4.41	7.7	99.2±0.65	33.1	262.3±9.73	87.4	241.2±2.25	80.4
400	32.9±1.51	8.2	105.7±4.61	26.4	305.3±24.8	76.3	302.1±1.51	75.5

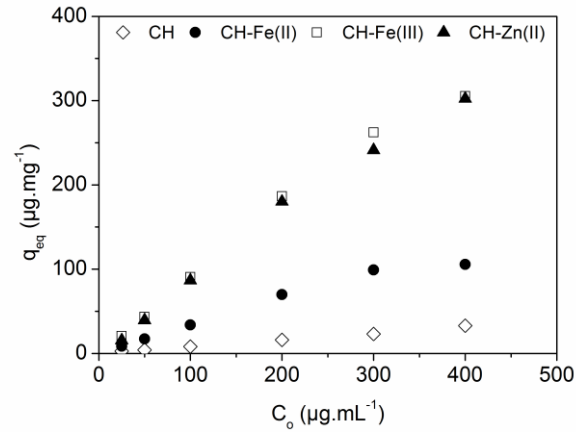


Figure 4: Adsorption capacity at equilibrium of ciprofloxacin by CH, CH-Fe(II), CH-Fe(III) and CH-Zn(II) microparticles as a function of ciprofloxacin initial concentration, in HEPES buffer (pH = 6.8, at 37°C).

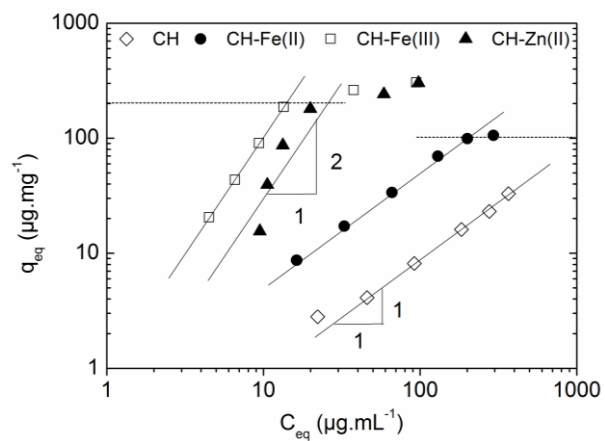


Figure 5: Adsorption isotherms of ciprofloxacin on CH, CH-Fe(II), CH-Fe(III) and CH-Zn(II) microparticles, in HEPES buffer (pH = 6.8, at 37°C). Dotted line represent the position of the adsorption saturation.

Table 3: Comparison of the first- and second-order rate constants and calculated and experimental  $q_{300}$  values obtained at different initial ciprofloxacin concentration for CH and CH-metal microparticles.

Microparticles	$C_o$ ( $\mu\text{g.mL}^{-1}$ )	$q_{300}$ ( $\mu\text{g.mg}^{-1}$ )	Pseudo-first-order kinetic			Pseudo-second-order kinetic		
			$K_{1,ad}$ ( $\times 10^{-3} \text{min}^{-1}$ )	$q_{300,1, calc}$ ( $\mu\text{g.mg}^{-1}$ )	$R_1^2$	$K_{2,ad}$ ( $\times 10^{-3} \text{mg} \mu\text{g}^{-1} \cdot \text{min}^{-1}$ )	$q_{300,2, calc}$ ( $\mu\text{g.mg}^{-1}$ )	$R_2^2$
CH	25	2.8	2.30	0.56	0.7579	25.15	1.83	0.9398
	50	4.1	12.20	0.73	0.6327	44.66	4.20	0.9967
	100	8.1	12.20	0.05	0.9638	0.49	13.64	0.3392
	200	16.1	4.83	0.04	0.8489	1.53	13.66	0.8965
	300	23.1	10.13	0.15	0.9663	0.61	24.44	0.8143
	400	32.9	11.05	0.18	0.9620	0.59	34.73	0.8739
CH-Fe(II)	25	8.71	2.76	0.25	0.7487	17.20	6.88	0.9961
	50	17.2	2.76	0.07	0.5627	9.34	13.56	0.9948
	100	33.8	2.30	0.001	0.2172	8.96	27.39	0.9879
	200	69.9	3.22	0.19	0.9907	1.24	54.34	0.9878
	300	99.2	4.60	0.18	0.7662	1.15	88.49	0.9903
	400	105.7	2.76	0.17	0.9236	1.78	90.09	0.9959
CH-Fe(III)	25	20.5	1.84	0.07	0.7232	10.99	15.87	0.9973
	50	43.4	2.07	0.16	0.9558	2.10	26.24	0.9840
	100	90.6	2.07	0.25	0.9452	0.81	54.05	0.9631
	200	196.5	1.61	0.33	0.9572	0.42	101.01	0.9680
	300	262.3	2.53	0.35	0.9222	0.29	169.49	0.9758
	400	305.3	24.64	0.48	0.8474	2.65	307.03	0.9490
CH-Zn(II)	25	15.5	6.22	0.07	0.9940	0.66	15.64	0.7373
	50	39.3	0.92	0.01	0.1068	2.07	30.30	0.9883
	100	86.7	4.37	0.14	0.6522	1.47	78.74	0.9891
	200	180.1	1.15	0.17	0.1009	4.44	153.84	0.9903
	300	262.3	3.22	0.33	0.7236	0.35	222.23	0.9669
	400	332.1	12.20	0.44	0.8153	0.01	326.31	0.9620

